

## Fermi Surface and Energy Bands of Copper

BENJAMIN SEGALL

General Electric Research Laboratory, Schenectady, New York

(Received August 16, 1961)

The Green's function method has been used to study the energy bands of Cu for two quite different potentials. It is found that the resulting  $E(\mathbf{k})$  for the two cases are very similar throughout the Brillouin zone having the same ordering of the levels and comparable level separations in the conduction, low-lying excited, and  $d$ -band regions. This implies that the calculated band structure is not as sensitive as had been previously contended. The properties of the Fermi surfaces associated with the two theoretical band structures are compared with the results of experimental studies. It is found that the theoretical surfaces intersect the hexagonal zone face in accord with experiment. The computed radii of contact for the two cases are close to the measured values. Furthermore, the bellies for the two cases are shown to deviate appreciably from sphericity in agreement with the results of recent

magnetoacoustic effect experiments. The origin of the distortions is explained in terms of the interaction between the conduction and  $d$  bands. The "masses" defined in terms of the cyclotron resonances for various orbits on the Fermi surface, the low-temperature electronic specific heat, and the dielectric constant in the infrared region are determined for the calculated  $E(\mathbf{k})$ . The calculated masses are all somewhat lower (by about 10–30%) than the corresponding measured masses. It is believed that these discrepancies reflect the contributions of the effects neglected in the individual-electron model. Finally, the sharp rise in the optical absorption, which on the basis of the theoretical  $E(\mathbf{k})$  corresponds to the onset of interband transitions between the  $d$  bands and the Fermi level, is found to occur at an energy in good accord with experiment.

### I. INTRODUCTION

FOR many years the electronic structure of metals has been the subject of both experimental and theoretical study. Our knowledge in this field has grown steadily, but in the last few years there has been a particularly rapid increase.<sup>1</sup> This has been primarily the result of the availability of high-purity materials, the development of new experimental techniques and the refinement of earlier methods. The methods referred to include the de Haas-van Alphen,<sup>2</sup> cyclotron resonance,<sup>3</sup> magnetoacoustic,<sup>4</sup> high-field magnetoresistance,<sup>5</sup> and anomalous skin effect measurements.<sup>6</sup> From these experiments a great deal of information about the geometry of the Fermi surface and the velocity for orbits on the surface can be obtained.<sup>7</sup>

On the theoretical side there has been considerable progress too. The formidable problems involving many-electron effects are being attacked with some success. For example, the important problem of showing theoretically that a "sharp" Fermi surface exists for systems of strongly interacting electrons has been carried out by Luttinger,<sup>8</sup> using perturbation theory to all orders. Similarly he has also shown how the theoretical results for some electronic properties are modified in the presence of interactions.

However, the inclusion of electron-electron interactions in a realistic theoretical investigation of a specific metal still appears to be a very formidable problem, and as a result the calculations are done at present within the framework of the individual particle, or band theory, model. In this area, there have been several powerful methods developed for studying the band structure of solids. The application of these methods has progressed to the point where, at present, the energy bands of a number of metals have been calculated accurately for an extensive sampling of the Brillouin zone.<sup>9</sup>

In terms of the experimental work the electronic properties of copper have been more thoroughly investigated than those of any other metal. As a result its electronic structure in the vicinity of the Fermi level is better known than for any other metal. Each of the experimental methods mentioned above has been extensively applied to the study of copper and the results have been found to fit one consistent and entirely reasonable picture of the Fermi surface. The surface that has emerged from these measurements is in a general way in accord with the model originally proposed by Pippard.<sup>10</sup> This model, which is shown in Fig. 1, consists of a central part (called the "belly"), which is roughly spherical like the free electron sphere, and eight "necks" which protrude from the belly and contact the hexagonal zone face of the Brillouin zone. In addition a good deal is known about the velocity,  $\mathbf{v}(\mathbf{k}) = \hbar^{-1} \nabla_{\mathbf{k}} E(\mathbf{k})$ , on the Fermi surface from the cyclotron resonance experiments.<sup>11</sup>

On the other hand, the theoretical situation for copper has been much less satisfactory. While there

<sup>1</sup> See Proceedings of the Fermi Surface Conference, Coopers-town, New York, August 22–24, 1960 [*The Fermi Surface*, edited by W. A. Harrison and M. B. Webb (John Wiley & Sons, Inc., New York, 1960)].

<sup>2</sup> D. Shoenberg, reference 1, p. 74; Phil. Mag. 5, 105 (1960).

<sup>3</sup> A. F. Kip, reference 1, p. 146.

<sup>4</sup> R. W. Morse, reference 1, p. 214.

<sup>5</sup> I. M. Lifshitz and V. G. Peschanskii, Soviet Phys.—JETP 8, 875 (1959); N. E. Alekseevskii and Yu. P. Gaidukov, *ibid.* 10, 481 (1960); R. G. Chambers, reference 1, p. 100; J. R. Klauder and J. E. Kunzler, J. Phys. Chem. Solids, 18, 256 (1961).

<sup>6</sup> See G. E. Smith, reference 1, p. 182, and references cited there.

<sup>7</sup> It must be recognized that the data obtained for metals with more complex surfaces, particularly those having several sheets, are generally so complicated that theoretical models are necessary as a guide to their interpretation.

<sup>8</sup> J. M. Luttinger, reference 1, p. 2.

<sup>9</sup> See J. Callaway, *Solid-State Physics*, edited by F. Seitz and D. Turnbull (Academic Press Inc., New York, 1958), Vol. 7, p. 99, which reviews the work up to 1958.

<sup>10</sup> A. B. Pippard, Phil. Trans. Roy. Soc. (London) A250, 325 (1957).

<sup>11</sup> A. F. Kip, D. N. Langenberg, and T. W. Moore, Phys. Rev. 124, 359 (1961).

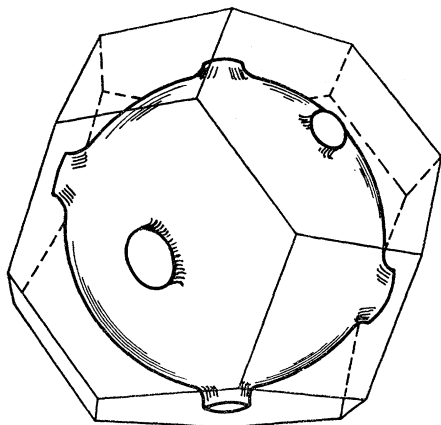


FIG. 1. A sketch of the Fermi surface of copper. The polyhedron represents the Brillouin zone.

have been several energy band calculations for this metal,<sup>12</sup> these have generally been restricted to only a few symmetry points (i.e., special  $\mathbf{k}$ 's) in the Brillouin zone. From this limited amount of information, most of the important facts about the Fermi surface that are of current interest, such as its shape and the effective masses for orbits on the surface, cannot be obtained. More serious, however, is that the results of previous calculations often badly conflicted with one another. This state of affairs led, in fact, to the widely-held belief that the calculated band structure of this and other metals having high-lying  $d$  levels (e.g., the other noble metals and the transition metals) are very sensitive to the details of the crystal potential employed. If true, this would lead to the very unsatisfactory conclusion that the results of such calculations could be highly questionable from the physical point of view.

The investigation of this question is one of the important motivations of this work. In order to study the question of the sensitivity of the results to the particular potential, we have made extensive calculations with two quite different but reasonable potentials.<sup>13</sup> In one, which was originally determined by Chodorow,<sup>14</sup> the potential is taken to be the same for all orbital angular momenta,  $l$ , while in the other the differences between the fields for different  $l$  are taken into account.

For these energy band calculations, we have used the Green's function method proposed by Kohn and Rostoker,<sup>15</sup> and independently, but from a different

point of view, by Korringa.<sup>16</sup> The various aspects of the method have recently been studied in detail<sup>17</sup> and the method has been applied in extensive calculations of the alkali metals<sup>18</sup> and aluminum.<sup>19</sup> The accuracy and convenience of this method have been demonstrated in these studies.

An important result of this work is that the  $E(\mathbf{k})$  for the two potentials are very similar throughout the zone so that the physical properties associated with the bands would be nearly the same for the two. On the basis of these results and a comparison with the earlier work, we believe that the difficulties encountered in the past were the result of inadequate solutions of the periodic potential problem and not of small differences in the force fields acting on the electrons as had been believed. Thus, aside from effects not included in the individual-particle framework, the results of a careful band study of this metal can be accepted with a reasonable amount of confidence.

The results of these calculations have also illustrated the point that, while the location of the  $d$  bands as a whole is somewhat affected by changes in the potential, the relative positions of the  $d$  levels with respect to each other are rather insensitive to the changes. The role that these bands play in affecting the conduction and low-lying bands is discussed.

The other principal reason for studying Cu is, of course, the wealth of available information about it. In this sense it is probably the best test for the band theory of metals. From a comparison of the band theoretical results with those determined empirically, it would be possible to determine to what degree a given aspect of the electronic structure is given correctly by band theory. This, of course, requires the use of an accurate (ideally a self-consistent) potential. While we cannot claim that the potentials employed in this work are self-consistent, they appear to be quite reasonable—particularly the second potential.

In Sec. IV we compare various electronic properties of Cu derived from the calculated energy band structures with those determined empirically. We find that the shape of the Fermi surface is given rather well by the band-theoretical results. Also, the onset of interband optical transitions indicated by the theoretical  $E(\mathbf{k})$  is in good accord with observation. We also consider the cyclotron resonance for several important orbits on the Fermi surface, the low-temperature electronic specific heat, and the dielectric constant for frequencies lower than those for the interband transitions. For each of these properties, a mass parameter is customarily introduced. The calculated values of these masses are all somewhat smaller (by about 10–30%) than the corresponding masses obtained from the experiments. The significance of these discrepancies in regards the

<sup>12</sup> Reference 9, p. 193.

<sup>13</sup> Most of the results and conclusions discussed in this paper were given in B. Segall and E. L. Kreiger, *Bull. Am. Phys. Soc.* **6**, 10 (1961) and in B. Segall, *ibid.* **6**, 231 (1961). The latter talk has been written up as General Electric Research Laboratory Report No. RL-2785G (unpublished). Also see B. Segall, *Phys. Rev. Letters* **7**, 154 (1961).

<sup>14</sup> M. Chodorow, *Phys. Rev.* **55**, 675 (1939); Ph.D. thesis, Massachusetts Institute of Technology, 1939 (unpublished). I wish to thank Dr. M. Saffren for bringing this reference to my attention.

<sup>15</sup> W. Kohn and N. Rostoker, *Phys. Rev.* **94**, 1111 (1954).

<sup>16</sup> J. Korringa, *Physica* **13**, 392 (1947).

<sup>17</sup> F. S. Ham and B. Segall, *Phys. Rev.* **124**, 1786 (1961).

<sup>18</sup> F. S. Ham (to be published).

<sup>19</sup> B. Segall, *Phys. Rev.* **124**, 1797 (1961).

validity of the band-theoretical treatment of these properties is discussed briefly.

## II. THE POTENTIALS

As mentioned in the previous section, the calculations have been carried out for two different potentials. The first was the one constructed by Chodorow over twenty years ago.<sup>14</sup> He, in effect, computed it by determining the "effective" field for the  $3d$  Hartree-Fock function for the free  $\text{Cu}^+$  ion. That is, he determined a field which when used in an ordinary Schrödinger equation (i.e., without an exchange operator) for  $l=2$  yielded a function which closely agreed with the  $3d$  Hartree-Fock function<sup>20</sup> for  $\text{Cu}^+$ . To this he added the contribution of a "metallic"  $s$  electron function which is the  $s$  function for an average energy. The use of this  $V(r)$  as the crystal potential involves, of course, invoking the Wigner-Seitz approximation. In this approximation it is assumed that all conduction electrons, except those for the unit cell under consideration, are excluded from the cell by the correlation and exchange interactions.

From the foregoing description, we can see that Chodorow's potential most closely represents the fields felt by a  $d$  electron. For this potential, as for most others employed in band calculations, the same potential is used for all angular momentum components of the wave function. This is done since a more general potential cannot be conveniently handled by most of the methods used for studying energy bands. In general the effective potential for the various  $l$  values differ, principally because of the different exchange contributions. In some cases, for example Al, Li, and Na, these differences are not too important. For Cu, however, we might expect some significant differences since the exchange contribution for a  $d$  electron, which is principally the exchange with the other nine  $d$  electrons and the one conduction electron, is definitely larger than the exchange interaction of one conduction ( $s$  or  $p$ ) electron with the ten  $d$  functions. There is also a difference which results from the fact that the Coulomb contribution of the former is for one conduction and nine  $d$  electrons while that for the latter is for ten  $d$  electrons.

Chodorow was aware of the fact that the potential might be inaccurate for  $l \neq 2$ , but he was primarily interested in the  $d$  bands for which the potential is quite reasonable. Now, the conduction states near  $E=E_F$  are largely  $s$  and  $p$  in character, and we are presently most interested in these states. Also, it is to be noted that the Green's function method, the one used for this work, can handle an  $l$ -dependent (i.e., operator) potential in a straightforward manner in contrast to other approaches.

With this in mind, we have attempted to determine a potential which more accurately reflects the differ-

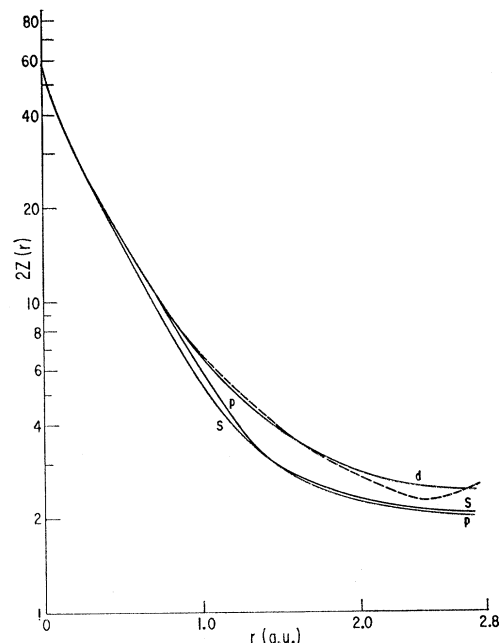


FIG. 2. The "charge"  $2Z_l(r) = -rV_l(r)$  for the crystal potentials used in the calculations. The  $V_l(r)$  is the  $l$ -dependent potential described in the text. The dashed curve is for Chodorow's potential.

ences in the fields experienced by the  $s$ ,  $p$ , and  $d$  electrons. To do this we used the core and  $d$ -electron Hartree-Fock functions for neutral copper<sup>21</sup> which were renormalized in the equivalent (or Wigner-Seitz) sphere. For the  $l=2$  potential, the Coulomb and exchange contributions were computed for a "configuration" which included in addition to the core and  $d$  electrons a renormalized  $s$  function. The  $s$  function was calculated for the "average" energy  $E(\Gamma_1) + \frac{2}{3}E_F$ , where the energy at the zone center  $E(\Gamma_1)$  and the Fermi energy  $E_F$  were estimated in advance. The estimated values were later proved to be sufficiently accurate for this purpose. The Coulomb and exchange contributions for  $l=0$  and  $1$  were also computed in a straightforward manner except that  $s$  and  $p$  functions for the estimated Fermi energy were used in evaluating the exchange integrals. This was done because we are most concerned about these functions for  $E \approx E_F$ . The potentials for  $l > 2$ , for which less accuracy is required, were taken to be equal to the  $l=0$  term. As for the other potential, the Wigner-Seitz approximation is used.

For comparison purposes, the functions  $2Z_l(r) = -rV_l(r)$ , where  $V_l(r)$  is the field for angular momentum  $l$ , are shown in Fig. 2. The corresponding expression for Chodorow's potential is also shown (dashed curve).

As indicated above, we believe that the second potential is somewhat more realistic than Chodorow's. Of course both potentials are approximate in a few

<sup>20</sup> D. R. Hartree and W. Hartree, Proc. Roy. Soc. (London) A157, 490 (1936).

<sup>21</sup> D. S. Story (private communication).

TABLE I. The energies for points of high symmetry for copper. The unit of energy is the rydberg.

State	Chodorow's $E(k)$	Present $E(k)$ , Chodorow's potential	$E(k)$ , present potential	$E(k) - E(\Gamma_1)$ , Chodorow's potential	$E(k) - E(\Gamma_1)$ , present potential
$\Gamma_1$	-1.041	-1.043	-0.836	0	0
$\Gamma_{25'}$	-0.649	-0.644	-0.505	0.399	0.331
$\Gamma_{12}$	-0.59	-0.584	-0.433	0.459	0.403
$X_1$	-0.76	-0.781	-0.666	0.262	0.170
$X_3$	-0.748	-0.745	-0.630	0.298	0.206
$X_2$	-0.546	-0.541	-0.383	0.502	0.453
$X_5$	-0.525	-0.526	-0.366	0.517	0.470
$X_{4'}$	-0.22	-0.224	-0.029	0.819	0.807
$X_1$		+0.169	+0.389	1.212	1.225
$L_1$	-0.77	-0.778	-0.646	0.265	0.190
$L_3$	-0.642	-0.648	-0.511	0.395	0.325
$L_3$	-0.528	-0.539	-0.380	0.504	0.456
$L_{2'}$	-0.43	-0.422	-0.247	0.621	0.589
$L_1$		-0.081	+0.189	0.962	1.025
$K_1$		-0.743	-0.620	0.300	0.216
$K_1$		-0.712	-0.587	0.331	0.249
$K_3$		-0.613	-0.463	0.430	0.373
$K_4$		-0.573	-0.419	0.470	0.417
$K_2$		-0.541	-0.384	0.502	0.452
$K_3$		-0.016	+0.168	1.027	1.004
$K_1$		+0.074	+0.254	1.117	1.090
$W_{2'}$		-0.726	-0.607	0.317	0.229
$W_3$		-0.673	-0.537	0.370	0.299
$W_1$		-0.585	-0.438	0.458	0.398
$W_{1'}$		-0.526	-0.365	0.517	0.471
$W_3$		+0.118	+0.310	1.161	1.146
$W_{2'}$		+0.258	+0.395	1.301	1.231
$W_1$		+0.294	+0.676	1.337	1.512

respects. Neither is self-consistent for the solid. Also, except for the crude correlation correction implicit in the Wigner-Seitz approximation, the many-electron aspects of the problem are neglected. The problem of how to include these correlation effects in the study of a real metal is, at present, one of the most important and challenging in the theory of solids.

The final approximation involved is the use of the "muffin-tin" potential form. A  $V(r)$  of this form is spherically symmetric inside the sphere inscribed in the polyhedral cell and is constant in the remainder of the cell. The constant value of the potential is taken to be equal to the average of the potential in the region of the cell outside the sphere. The constant value for Chodorow's potential is  $-0.937$  ry and that for the second potential is  $-0.900$  ry. The use of the muffin-tin

potential involves a relatively small error as we will later show.

It is, of course, true that it is very difficult to estimate the magnitude of the errors associated with the first two of the three approximations discussed above. However, it is our belief, based on the present and past band theoretical studies, that the general features of the electronic structure are given correctly by the results of an accurate energy band calculation. The test of the validity of this belief will be the comparison of the results of calculation with experiment. As mentioned in the previous section, Cu is at present the ideal metal to test.

### III. THE CALCULATED ENERGY BANDS

Before going on to the results of the calculations, it is desirable to remind the reader of the Brillouin zone for the face-centered cubic structure. This is shown in Fig. 3 in which the points and lines of high symmetry are indicated. In this work we will use Bouckaert, Smoluchowski, and Wigner's<sup>22</sup> notation for the irreducible representations associated with these points and lines. The eigenvalues for points along these axes have been calculated along with points in a (110) plane. The free electron Fermi sphere for copper comes out about 0.90 of the way from the center of the zone,  $\Gamma$ , to the nearest point on the zone surface,  $L$ .

The energy levels in the conduction, low-lying

<sup>22</sup> L. P. Bouckaert, R. Smoluchowski, and E. Wigner, Phys. Rev. 50, 58 (1936).

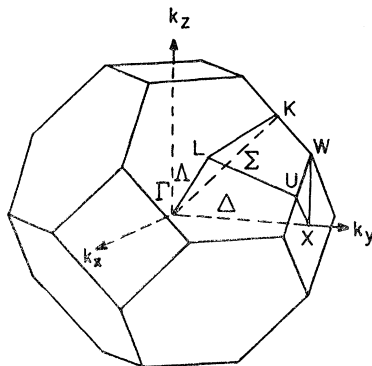


FIG. 3. The Brillouin zone for the face-centered cubic structure with points and lines of high symmetry.

excited, and  $d$ -band regions for all the principle symmetry points [i.e.,  $\Gamma$ ,  $L$ ,  $X$ ,  $K(U)$ , and  $W$ ] are given in Table I. In the third column we have tabulated the eigenvalues for Chodorow's potential. These are to be compared with the energies obtained by Chodorow<sup>14</sup> using Slater's augmented plane wave method.<sup>23</sup> His results, which were limited to the symmetry points  $\Gamma$ ,  $X$ , and  $L$ , are listed in the second column. It can be seen that the two sets of eigenvalues are in very good accord. Except for the lower  $X_1$  level for which his result is given to two figures only and where the results differ by 0.02 ry, the two sets of energies deviate from each other by less than 0.01 ry.

More recently Burdick<sup>24</sup> has also calculated the  $E(\mathbf{k})$  for Chodorow's potential using the augmented plane wave method. His eigenvalues for all the symmetry points in the zone are found to agree very closely with our values for the same potential.

The symmetry point  $E(\mathbf{k})$ 's for the  $l$ -dependent potential are given in the fourth column of Table I. As it is more meaningful and convenient to compare the relative energies, the symmetry point energies with respect to the  $\Gamma_1$  level are given in the fifth and sixth columns for Chodorow's and the second potential, respectively.

The most important feature of the comparison of the relative  $E(\mathbf{k})$ 's for the two potentials is their very close similarity for all the symmetry points. The ordering of all the levels for a given symmetry point is identical for both. Further, the level separations are nearly the same. This, of course, implies that the band structure for both of these quite different potentials are very similar throughout the Brillouin zone. Our calculations for more general  $\mathbf{k}$ , to be discussed below, will illustrate this more graphically.

A closer comparison of eigenvalues provides an illustration of the fact that by using for the  $s$  and  $p$  components the  $V(r)$  which is appropriate for the  $d$  electrons, one is, in effect, including too large an interaction for  $l \neq 2$ . This is most easily seen for the states at  $\Gamma$  where the complicating effects of the interaction between the  $s$  and  $d$  bands do not enter. There we see first that the  $d$ -state separation,  $E(\Gamma_{12}) - E(\Gamma_{25'})$ , is very close for the two cases. On the other hand, the  $s$  state,  $\Gamma_1$ , is depressed with respect to  $d$  levels about 0.06 ry more for Chodorow's than for the  $l$ -dependent potential, in which the differences in the fields for the various  $l$  are treated more appropriately.

To illustrate the nature of the energy bands for copper we show, in Fig. 4, the  $E(\mathbf{k})$  for the  $l$ -dependent potential for  $\mathbf{k}$  along the  $\langle 111 \rangle$  axis. The bands for a free electron (dashed curves) are also given in this figure. The differences between the  $E(\mathbf{k})$  for copper and the free electron are quite marked. First of all, the  $d$  bands—which might be defined as the states in the

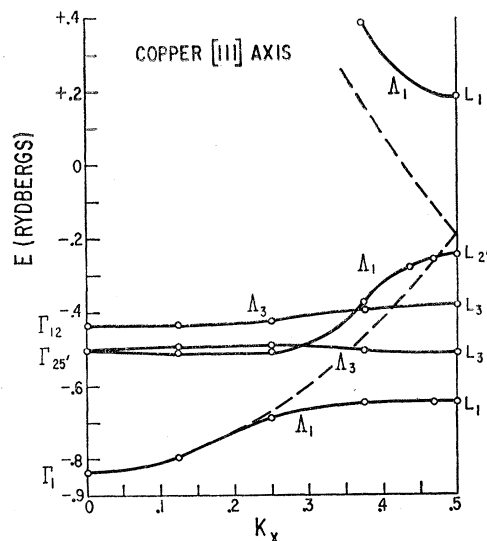


FIG. 4. The calculated energy bands for Cu along the  $\langle 111 \rangle$  axis for the  $l$ -dependent potential.

energy range from around the lowest  $L_1$  to the upper  $L_3$  state—lie practically in the middle of the first free electron band. The other point in which they differ greatly is that for the real metal there is a large gap at  $L$  [i.e.,  $E(L_1) - E(L_{2'})$ ].

With these features in mind we can better understand Figs. 5 and 6 in which the  $E(\mathbf{k})$  for Chodorow's and the second potential are shown for the various symmetry axes within the Brillouin zone and on the zone surface. For comparative purposes we show in Fig. 7 the corresponding bands for a free electron (dashed curves) and for the metal aluminum,<sup>19</sup> which also has the face-centered structure. We note that in marked contrast to Cu, Al has bands which bear a striking resemblance to those of a free electron. The essential difference between its  $E(\mathbf{k})$  and that of the free electron is the small splittings of the specifically free-electron degeneracies.

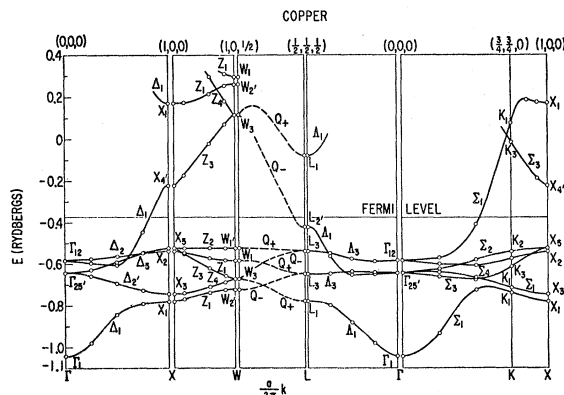


FIG. 5. The calculated energy bands for Cu along the various symmetry axes in the Brillouin zone and on the zone surface for Chodorow's potential.

<sup>23</sup> J. C. Slater, Phys. Rev. **51**, 846 (1937).

<sup>24</sup> G. A. Burdick, Phys. Rev. Letters **7**, 156 (1961).

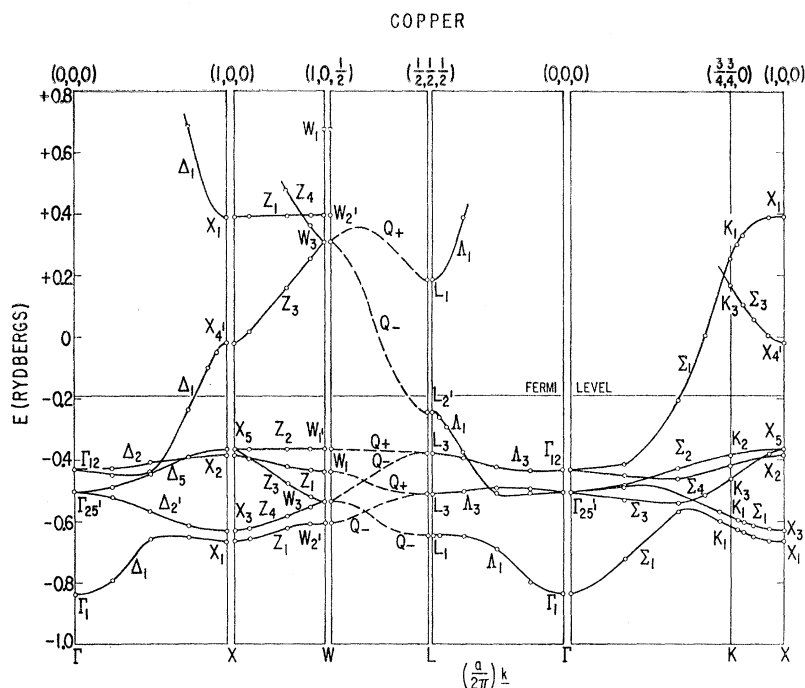


FIG. 6. The calculated energy bands for Cu along the various symmetry axes in the Brillouin zone and on the zone surface for the  $l$ -dependent potential.

We will comment only on the general characteristics of the energy bands depicted in Figs. 5 and 6. As we would expect from our discussion of the symmetry point energies, the  $E(\mathbf{k})$  for the two cases are indeed very similar throughout the Brillouin zone. The similarity between the  $d$  bands for the two is particularly striking. The major difference is that the  $s$  and  $p$  levels for Chodorow's potential are generally about 0.2 ry lower than those for the second potential and the  $d$  levels about 0.12–0.14 ry lower. This, of course, directly reflects the differences in the potentials which are evident in Fig. 2. The region of importance for the  $s$  and  $p$  electrons is from about  $r=2.0$  to 2.7 atomic units (a.u.), and there the potential for  $l=0$  and 1 is weaker than Chodorow's by roughly 0.2 ry. For the case of the  $d$  electrons, the crucial region is in the neighborhood of  $r=1$  a.u. near where the  $l=2$  wave function peaks. Here the  $d$  potential is weaker than Chodorow's by about 0.1 ry.

For both cases, the  $d$  bands lie in the middle of the first free electron band throughout the zone. The widths of the  $d$  band are about 3.5 ev and 4.1 ev for the  $E(\mathbf{k})$ 's based on Chodorow's and the  $l$ -dependent potential, respectively. Also there are large gaps at  $X$  and  $L$  with the  $p$ -like states,  $X_4'$  and  $L_2'$ , lower than the  $s$ -like states,  $X_1$  and  $L_1$ , for both cases. The gap at  $L$  is 4.6 ev for the first and 5.9 ev for the second case.<sup>25</sup>

There is another feature of the bands which has

important implications for the nature of the Fermi surface. For a given  $|\mathbf{k}|$ , the conduction band state in the  $\langle 110 \rangle$  direction ( $\Sigma_1$ ) has a higher energy than that in the  $\langle 100 \rangle$  direction ( $\Delta_1$ ) which in turn lies higher than the state in the  $\langle 111 \rangle$  direction ( $\Lambda_1$ ). As this fact cannot be seen easily in the other curves, the energies for the  $\Sigma_1$ ,  $\Delta_1$ , and  $\Lambda_1$  conduction band states are plotted in Fig. 8 as a function of  $|\mathbf{k}|$  for both potentials.

All of the results presented so far have been obtained for potentials of the "muffin-tin" form,  $V_{m.t.}(\mathbf{r})$ . As the question of the effect of using this approximation often arises, we will estimate the shifts of the  $L_2'$ ,  $L_1$ ,  $X_4'$ , and  $X_1$  levels due to  $\delta V(\mathbf{r}) = V(\mathbf{r}) - V_{m.t.}(\mathbf{r})$  using first-order perturbation theory. Since the procedure for carrying this out has been given elsewhere,<sup>17,19</sup> it will not be repeated here. We will note only that, as one might expect and as we have demonstrated for Al, almost the entire perturbation comes from the regions outside the inscribed sphere.<sup>19</sup>

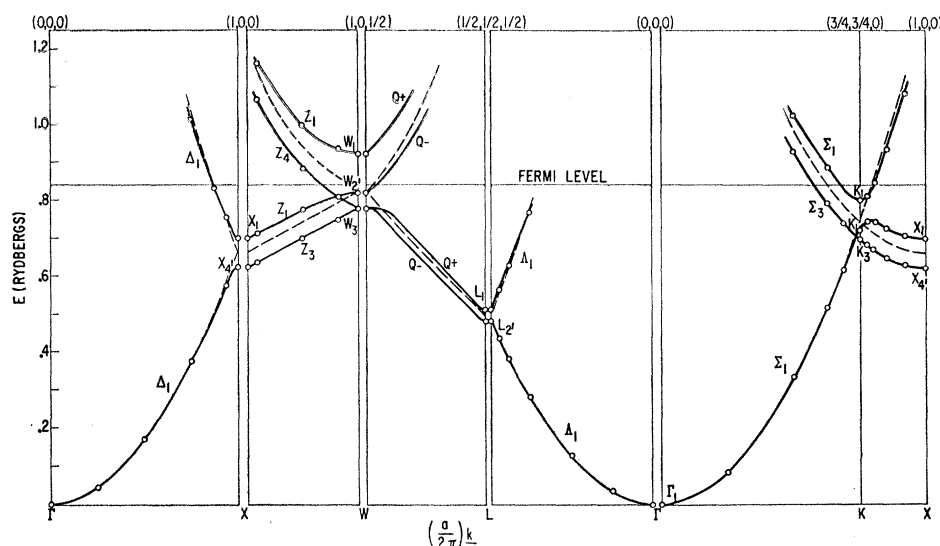
The perturbing potential, which arises primarily from the fields of the near neighbors, cannot be determined simply from the approach used in Sec. II. To estimate  $\delta V(\mathbf{r})$  we take the total  $V(\mathbf{r})$  to be given by a superposition of potentials centered at the atomic sites, i.e.,  $\sum_i U(|\mathbf{r} - \mathbf{R}_i|)$ . The  $U(\mathbf{r})$  are taken to be the fields for the neutral atoms with the total charge of each being normalized to an equivalent sphere. A term, calculated by Behringer,<sup>26</sup> was added to correct for the fact that the charge density is not properly represented by a distribution of charges confined within the equivalent sphere.

The resulting first-order shifts of the levels being

<sup>25</sup> It is interesting to note that in their attempts to fit the Fermi surface using admittedly rough models of the energy bands, both A. B. Pippard, reference 10, and J. M. Ziman, *Advances in Physics*, edited by N. F. Mott (Taylor and Francis, Ltd., London, 1961), Vol. 10, p. 1, concluded that the gap at  $L$  is large. Their values are, in fact, somewhat larger than we have found.

<sup>26</sup> R. E. Behringer, *J. Phys. Chem. Solids* **5**, 145 (1958).

FIG. 7. The energy bands for a free electron (dashed curve) and for Al for the various symmetry axes in the Brillouin zone and on the zone surface.



considered are  $\Delta E(L_{2'}) = \Delta E(X_1) = -\Delta E(X_{4'}) = 0.004$  ry and  $\Delta E(L_1) = -0.003$  ry. It is seen that the perturbations are indeed small. The  $d$  levels would be perturbed even less since their wave functions are much smaller in the corners of the polyhedral cell than are those for the states just considered.

Before concluding our discussion of the energy band calculations, it would be interesting to compare them with some of the previous results in the literature. This is important because as a result of the bad discrepancies among some of the earlier results, considerable doubt was raised as to the value of such calculations for metals like Cu.

In Table II we have listed the conduction and first excited band energies obtained in most of the published calculations on Cu. To facilitate the comparison all energies are given with respect to the  $\Gamma_1$  level. It is apparent that there are a number of significant discrepancies. Perhaps the most glaring differences are seen in the orderings of the  $s$  and  $p$  levels for the gaps at  $X$  and  $L$ . In the works of Tibbs,<sup>27</sup> Howarth (1953),<sup>28</sup>

and Howarth (1955),<sup>29</sup> the  $s$ -like state  $L_1$  is found to lie lower than the  $p$ -like state  $L_{2'}$ , in marked disagreement with the results discussed earlier and with those of Fukuchi.<sup>30</sup> The  $X_1$  state ( $s$ -like) is also lower than the  $X_{4'}$  state ( $p$ -like) in Howarth's 1955 results, and while the order is the opposite in his 1953 work the separation of the levels,  $E(X_1) - E(X_{4'})$ , is very much smaller than that found in the present and in Fukuchi's work.

Of these previous studies it is apparent that Fukuchi's results for the symmetry point eigenvalues, obtained by the OPW method, most closely agree with our results. The agreement is better for the states with  $p$  character than those with  $s$  symmetry. It is to be noted that Fukuchi also calculated the  $E(\mathbf{k})$  along the  $\langle 100 \rangle$ ,  $\langle 111 \rangle$ , and  $\langle 110 \rangle$  axes and found rather free electron-like bands connecting the  $\Gamma_1$  level to those on the zone surface. This is, of course, incompatible with our  $E(\mathbf{k})$  (see Figs. 5 and 6) and results from his neglect of the  $d$  bands. This neglect is probably also responsible for the fact that his  $s$ -like states are lower than ours. This

TABLE II. Energies for the conduction band and first excited band states obtained in earlier calculations. The energies are given relative to the  $s$  state at the center of the zone,  $\Gamma_1$ , in rydbergs.

	Tibbs <sup>a</sup>	Howarth (1953) <sup>b</sup>	Howarth (1955) <sup>c</sup>	Fukuchi <sup>d</sup>
$L_{2'}$	0.64	0.78	0.680	0.586
$L_1$	0.43	0.651	0.576	0.889
$X_{4'}$		0.80	0.856	0.783
$X_1$		0.84	0.729	1.174
$K_3$			0.449	0.938
$K_1$			0.440	1.022

<sup>a</sup> See reference 27. The energies are interpolated to the observed lattice constant.

<sup>b</sup> See reference 28. The results for the Hartree-Fock potential are quoted.

<sup>c</sup> See reference 29. The results for the Hartree-Fock potential are quoted.

<sup>d</sup> See reference 30.

TABLE III. Energies for the  $d$  band states obtained in earlier calculations in rydbergs.

	Howarth (1953) <sup>a</sup>	Howarth (1955) <sup>b</sup>
$\Gamma_{12}$	-0.195	-0.155
$\Gamma_{25'}$	-0.235	-0.054
$X_1$	-0.12	-0.335
$X_2$	-0.13	-0.106
$X_3$	-0.344	-0.074
$X_5$	-0.088	-0.066
$L_1$	-0.248	-0.276
$L_3$		-0.146
$L_{3'}$		-0.065

<sup>a</sup> See reference 28.

<sup>b</sup> See reference 29.

<sup>27</sup> S. R. Tibbs, Proc. Cambridge Phil. Soc. 34, 89 (1938).

<sup>28</sup> D. J. Howarth, Proc. Roy. Soc. (London) A220, 513 (1953).

<sup>29</sup> D. J. Howarth, Phys. Rev. 99, 469 (1955).

<sup>30</sup> M. Fukuchi, Progr. Theoret. Phys. (Kyoto) 16, 222 (1956).

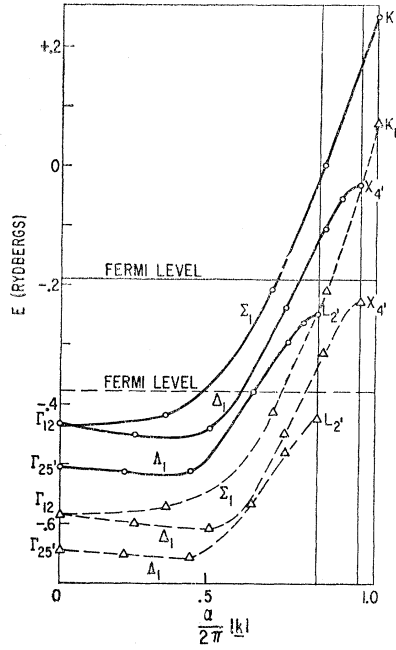


FIG. 8. The Cu conduction band states  $\Delta_1$ ,  $\Delta_2$ , and  $\Sigma_1$  for the  $\langle 111 \rangle$ ,  $\langle 100 \rangle$ , and  $\langle 110 \rangle$  directions, respectively. The solid curves represent the bands for the  $l$ -dependent potential and the dashed curves those for Chodorow's potential.

comes about because the conduction and excited states "interact" with the  $d$ -band states in such a way that the  $s$  states are pushed upwards. This "interaction" will be discussed below.

Of these earlier investigations, the only ones beside Chodorow's in which the  $d$  bands were studied were Howarth's 1953 and 1955 calculations. The results for these are given in Table III. Comparing the relative positions of these levels among themselves with the corresponding separations in Table I, we find fair agreement for several and appreciable disagreement for the others.

We have already commented on the general agreement of the  $E(\mathbf{k})$  for the second potential and Chodorow's. In our discussion above, we also noted the reasonably good accord with Fukuchi's energies obtained with still another potential and by another method. As mentioned above, the agreement would be still better had he taken the  $d$  states into account. From these comparisons, and from our experience with other calculations, we conclude that the energy bands are *not* extremely sensitive to the details of the potentials as had been contended in the past. It appears that the earlier discrepancies must have been due to inadequate methods of solving the periodic potential problem or to the improper application of accurate methods.

We are, of course, not contending that differences in the potentials are completely unimportant, but merely that small differences in the  $V(\mathbf{r})$ 's lead to only small changes in the eigenvalues. We have, for example, shown that the use of the muffin-tin potential leads to shifts of about 0.005 ry. By far the most sensitive feature of the calculations of metals like Cu is the

position of the  $d$  bands as a whole with respect to the other levels. But the present work shows that even this can be given without too great an uncertainty by the use of a reasonable potential. This will be borne out in the next section where we compare the consequences of these results with experimental findings.

#### IV. COMPARISON WITH EXPERIMENT

##### The Shape of the Fermi Surface

The geometry of the Fermi surface for copper has been studied or, at least in some aspects, checked by all of the experimental methods noted in Sec. I and as a result it is probably the best known aspect of the electronic structure. It thus provides one of the most crucial checks for the calculated energy bands.

As indicated in Fig. 8, the conduction band is far from spherically symmetric and it has its lowest energy along the  $\langle 111 \rangle$  axis. This relative depression of the conduction band in the  $\langle 111 \rangle$  direction is the property of the energy bands that is required in order for the Fermi surface to contact the zone surface in the vicinity of the point  $L$  [i.e.,  $\mathbf{k}_L = (2\pi/a)(\frac{1}{2}, \frac{1}{2}, \frac{1}{2})$ ].

We wish, however, to establish this point more conclusively. Also, we want to determine the Fermi level  $E_F$  and the parameters characterizing the Fermi surface quantitatively. This, of course, could be accomplished directly by calculating the  $E(\mathbf{k})$  at a large number of general points in the zone to obtain constant energy surfaces and the density of states. It is possible to avoid this by using two simple approximations. First we employ the simple expression

$$E(\mathbf{k}) = \hbar^2 \mathbf{k}_\perp^2 / 2m^* + E(\mathbf{k}_\parallel), \quad (1)$$

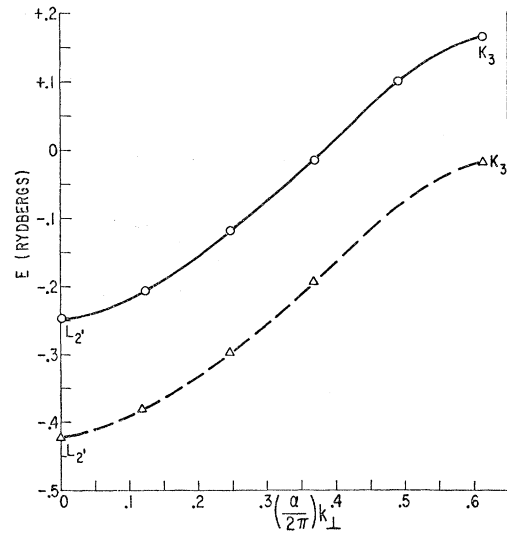


FIG. 9. The calculated conduction band for Cu on the intersection of a  $\langle 110 \rangle$  plane and the hexagonal zone face. The abscissa  $k_\perp$  is the component of  $\mathbf{k}$  lying in the hexagonal face. The solid curve gives the  $E(\mathbf{k})$  for the  $l$ -dependent potential and the dashed curve that for Chodorow's potential.



TABLE IV. The theoretical and experimental "neck" and average "belly" radii for the Fermi surface of copper. The theoretical values are given for the band structures based on the two potentials used in this work. The values tabulated for the de Haas-van Alphen experiments are the radii of circular cross sections having areas equal to those obtained from the measurements. All the tabulated wave vectors are given in units of  $10^8 \text{ cm}^{-1}$ . For comparison the radius of the free electron sphere is  $1.365 \times 10^8 \text{ cm}^{-1}$ .

	Fermi surface, Chodorow's potential	Fermi surface, present potential	Experimental
"Neck radius"	$0.20 \pm 0.03$	$0.28 \pm 0.03$	$0.26^a$ $0.28^{bc}$
Average "belly" radius	$1.35 \pm 0.02$	$1.33 \pm 0.01$	$1.38^{bc}$ ( $H \parallel \langle 111 \rangle$ ) $1.40^{bc}$ ( $H \parallel \langle 100 \rangle$ )

<sup>a</sup> See reference 31.

<sup>b</sup> See reference 2.

<sup>c</sup> See Note added in proof.

to give the energy for  $\mathbf{k}$  in the neighborhood of  $L$ . In Eq. (1)  $\mathbf{k} = \mathbf{k}_L + \mathbf{k}_{11}$  where  $\mathbf{k}_L$  and  $\mathbf{k}_{11}$  are the components of the wave vector perpendicular and parallel to the  $\langle 111 \rangle$  axis, and  $m^*$  represents the effective mass for motion transverse to the axis. One can show, using the  $\mathbf{k} \cdot \mathbf{p}$  perturbation approach, that Eq. (1) is correct up to fourth-order terms in the components of  $\mathbf{k} - \mathbf{k}_L$ . As we will require Eq. (1) only for small  $\mathbf{k} - \mathbf{k}_L$ , it is evident that the expression is very accurate.

In order to fit the effective-mass parameter entering Eq. (1), the conduction band energies for  $\mathbf{k}$  on the intersection of a  $\langle 110 \rangle$  plane and the hexagonal face have been calculated. These  $E(\mathbf{k})$ , which connect the  $L_{2'}$  levels to the  $K_3$  levels, are shown for both potentials in Fig. 9. The masses obtained by fitting the bands near the Fermi levels, which are close to the  $L_{2'}$  levels, are  $0.4 m_0$  in both cases.

In the other approximation we take the volume of the belly to be that of a sphere with a radius  $\bar{k}$  which is the mean of the wave vectors in the  $\langle 100 \rangle$  and  $\langle 110 \rangle$  directions. We have already noted that the calculated belly is not very spherical; but from what we will learn about the shape of the Fermi surface we can see that the approximation is not unreasonable. We would judge that this approximation might lead to an error of a few percent (say 3–5%) in the volume of the belly. The estimated error associated with the use of Eq. (1) is less than this.

On the circle at which the neck joins the belly, the relation  $\bar{k}^2 = \mathbf{k}_L^2 + \mathbf{k}_{11}^2$  is satisfied. From this and Eq. (1), the limits of  $\mathbf{k}_{11}$  for the neck region are found for a given energy. The neck volume is then obtained by a straightforward integration. By adding the volume of the eight necks to that of the sphere and making a small correction for the eight spherical caps which have been included twice, the total volume within the constant energy surface is evaluated. The Fermi energy  $E_F$  is then determined by the requirement that the enclosed volume equal one-half the volume of the Brillouin zone so that the correct number of states are occupied.

By this means the  $E_F$  associated with the energy bands for the  $l$ -dependent potential was found to be  $-0.183 \pm 0.010 \text{ ry}$  while that for Chodorow's potential

is  $-0.385 \pm 0.010 \text{ ry}$ . The ranges of uncertainty indicated for these  $E_F$  result from the estimated uncertainty in the belly volume.

Since the calculated  $E_F$  levels for both potentials lies higher than the energies of the  $L_{2'}$  states, the Fermi surfaces for both intersect the zone surface. Further, the radius with which the neck contacts the zone surface,  $k_N$ , can readily be found from Fig. 9 or from Eq. (1) for  $E(\mathbf{k}) = E_F$  and  $\mathbf{k}_{11} = \mathbf{k}_L$ . The calculated neck radii,  $k_N$ , the average belly radii,  $k_B$ , for the two band structures are given in Table IV, along with the corresponding values obtained from the de Haas-van Alphen effect<sup>2</sup> and magnetoacoustic effect<sup>31</sup> measurements. The measured period in  $1/H$  of the de Haas-van Alphen oscillations is related to the Fermi surface by the relation  $P = 2\pi e / \hbar c \mathcal{Q}$ , where  $\mathcal{Q}$  is an extremal cross-sectional area normal to the magnetic field. The radii tabulated for these measurements are defined in terms

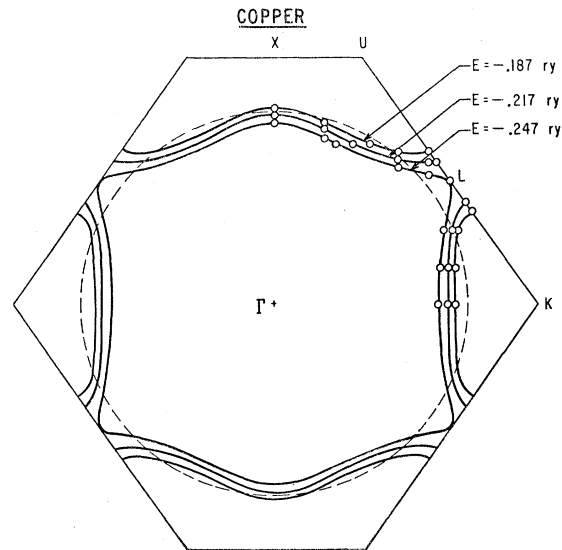


FIG. 10. The intersections of a  $\langle 110 \rangle$  plane with the surfaces of constant energy for Cu for the  $l$ -dependent potential. The estimated Fermi energy is  $-0.183 \pm 0.010 \text{ ry}$ . The dashed curve is the intersection with the free-electron sphere.

<sup>31</sup> R. W. Morse, A. Myers, and C. T. Walker, J. Acoust. Soc. Am. 33, 699 (1961).

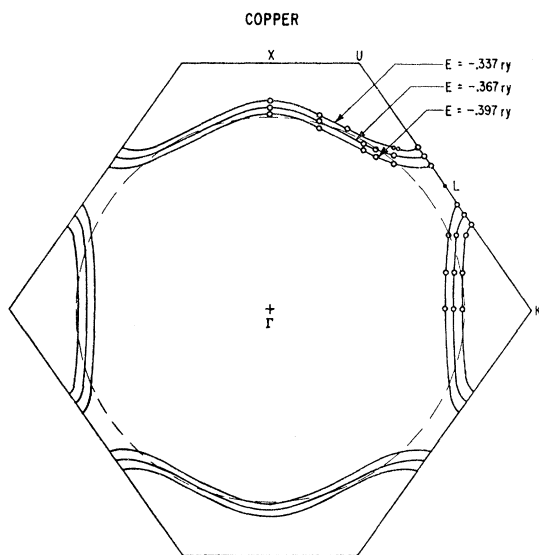


FIG. 11. The intersections of a (110) plane with the surfaces of constant energy for Cu for Chodorow's potential. The estimated Fermi energy is  $-0.385 \pm 0.010$  ry. The dashed curve is the intersection with the free-electron sphere.

of equivalent circular cross-sectional areas. It is seen that both of the calculated  $k_N$ 's agree fairly well with the two different experimental values. It is to be noted that the de Haas-van Alphen values for  $k_B$  are not only higher than the theoretical values but are larger than the free electron sphere radius  $k_F$ . It is difficult to understand why these values should not be less than  $k_F$  by a few percent because of the finite fraction of the volume (about 5-10%), within the eight necks. This discrepancy, evidently, cannot be attributed to many-electron effects for Luttinger<sup>32</sup> has shown that the volume within  $E(\mathbf{k}) = E_F$  is not altered when the electron-electron interactions are taken into account. Thus, if the experimental values are too large to this extent, as appears to be the case, there would be no appreciable disagreement with the calculated values.<sup>32a</sup>

On the basis of his recently obtained  $E(\mathbf{k})$  for Chodorow's potential, Burdick<sup>24</sup> has also studied the shape of the Fermi surface. His results appear to be similar to ours.

The final aspect of the shape of the Fermi surface that we will discuss are the energy contours in a (110) plane. A few of these are shown for the  $l$ -dependent potential in Fig. 10 and for Chodorow's potential in Fig. 11. In Fig. 10 the contour for the estimated  $E_F$  is close to the curve for the highest energy, while in Fig. 11 it is between the two lowest energy curves. The general features of the shape of the surfaces are clearly the same in both cases. The most interesting feature of these curves, aside from the substantial region of contact for  $E = E_F$ , is the fact that we find that the bellies of these Fermi surfaces are not nearly as spherical

as was found by Pippard<sup>10</sup> using the anomalous skin effect. These surfaces tend to be pulled out along the  $\langle 100 \rangle$  axes and pushed in along the  $\langle 110 \rangle$  axes. This particular distortion effect has recently been observed by Morse *et al.*<sup>31</sup> using the magnetoacoustic effect. While they do not present any numerical values for the main section of the surface, it is clear from their Fig. 1 that not only are the calculated distortions in the same direction but that they are of the same magnitude as the observed ones. It should be noted that Pippard's surface exhibits distortions in the same direction but of a smaller magnitude (about  $\frac{1}{3}$  of the present ones).<sup>32a</sup>

These distortions result from the fact mentioned earlier, that for a given  $|\mathbf{k}|$  the conduction band states along the  $\langle 110 \rangle$  direction is higher than that along the  $\langle 100 \rangle$  direction (see Fig. 8). We will see that this in turn is related to the occurrence of relatively high-lying  $d$  bands in this metal and their interactions with the other bands.<sup>33</sup> The conduction bands are selectively "repelled" by the  $d$ -band states of the same symmetry through an admixture of  $d$  component in their wave functions. Since the lowest conduction band state at the end of  $\langle 100 \rangle$  axis has  $X_{4'}$  ( $p$ -like) symmetry, and since this symmetry cannot occur for the  $d$  bands, this state is not repelled. The states near  $X_{4'}$  will have only a small admixture of  $l=2$  component and will consequently only weakly "interact" with the lower bands. The states for the  $\langle 110 \rangle$  direction, on the other hand, will interact fully with the  $d$  bands all the way out to the zone surface. As a result the  $\Sigma_1$  states will lie higher than the  $\Delta_1$  states for the same  $|\mathbf{k}|$ .

This argument applies equally well to the other noble metals for as we have shown elsewhere the ordering of the conduction band states is the same for them as for Cu.<sup>34</sup> It is noteworthy that these deviations from sphericity have also been observed in Au.<sup>31</sup> Silver has not as yet been investigated as thoroughly as the other two because samples of sufficiently high purity have not been available.

### Cyclotron Masses

Through the cyclotron resonance studies a great deal of knowledge has been obtained of the derivative properties of the Fermi surface, that is, the difference between neighboring constant energy surfaces for  $E \approx E_F$ . In their extensive investigations on Cu, Kip, Langenberg, and Moore<sup>11</sup> have determined the cyclotron masses for many of the various possible orbits on the Fermi surface.

The cyclotron mass  $m_c$ , for a given orbit, is defined by

$$m_c = \hbar (2\pi)^{-1} \oint d\mathbf{k} v_1^{-1}, \quad (2)$$

<sup>32</sup> J. M. Luttinger, Phys. Rev. **119**, 1153 (1960).

<sup>32a</sup> See Note added in proof.

<sup>33</sup> For example, see M. Saffren, reference 1, p. 341.

<sup>34</sup> B. Segall, Bull. Am. Phys. Soc. **6**, 145 (1961); **6**, 231 (1961).

where  $v_{\perp}$  is the component of the velocity normal to the magnetic field and the integral is taken around the orbit. This can readily be transformed into<sup>36</sup>

$$m_c = \frac{\hbar^2}{2\pi} \frac{\partial A(k_H)}{\partial E} \bigg|_{E_F}, \quad (3)$$

where  $A(k_H)$  is cross-sectional area of the Fermi surface in the plane  $k_H = \text{constant}$ , which is perpendicular to magnetic field  $H$ .

The cyclotron masses for a few of the principal orbits have been calculated. The orbit for which we can compute  $m_c$  most accurately is the "dog's bone" orbit which is illustrated in Fig. 12(b). The velocity for this orbit, which occurs for  $H$  in a  $\langle 110 \rangle$  direction, can be obtained from the energy contours in the  $(110)$  plane that we have already obtained (see Figs. 10 and 11). Using either Eq. (2) or (3) we obtain the values  $m_c = (1.13 \pm 0.06)m_0$  and  $(1.12 \pm 0.06)m_0$  for the case of Chodorow's and the  $l$ -dependent potential, respectively. The measured mass is  $(1.24)m_0$ .<sup>11</sup>

The extremal belly orbit for  $H$  in the  $\langle 100 \rangle$  direction is shown in Fig. 12(a). As we have not calculated the energy contours for the  $(100)$  plane, we cannot compute the velocity all along the orbit. We can, however, compute the velocities along the  $\langle 100 \rangle$  and the  $\langle 110 \rangle$  axes. We find from these and from the values at other points on the belly, that  $\mathbf{v}(\mathbf{k})$  does not vary much over the main part of the surface. It is then possible to evaluate Eq. (2) by using an average value of  $v_{\perp}$  for the orbit, which is taken to be the mean of  $v_{\perp}$  for the  $\langle 100 \rangle$  and  $\langle 110 \rangle$  axes. For the path length we take the value  $2\pi k_B$ . By this means we arrive at the mass value of  $m_c = (1.2 \pm 0.1)m_0$  for the first and  $(1.1 \pm 0.1)m_0$  for the second band structures. The experimental value is  $1.38 m_0$ .<sup>11</sup>

To evaluate the mass for orbits about the neck we make use of the fact that the energy contours on the hexagonal face must have hexagonal symmetry, and thus must then be rather circular. This approximation is consistent with Eq. (1) which, as we noted earlier, is quite accurate for small  $\mathbf{k} - \mathbf{k}_L$ . With this approximation, the neck mass can readily be calculated, and the values that we find for it are  $(0.39 \pm 0.02)m_0$  for the case of Chodorow's and  $(0.41 \pm 0.02)m_0$  for the case of the second potential. This is close to the same value as was found before for the effective mass  $m^*$  used in Eq. (1), and results from the nearly parabolic dependence of  $E(\mathbf{k})$  on  $\mathbf{k}_L$ . For comparison, the experimental neck mass is found to be  $0.6 m_0$ .<sup>11</sup>

As we can see, the agreement between the calculated and measured cyclotron masses is only semi-quantitative. The calculated values are all lower (by about 10–30%) than the experimentally determined values. It is interesting to note that similar discrepan-

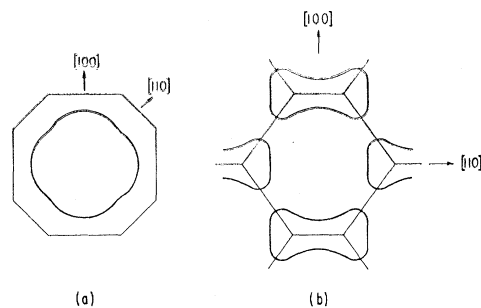


FIG. 12. Two orbits on the Fermi surface of Cu. The drawing (a) represents the extremal "belly" orbit for  $H \parallel \langle 100 \rangle$  and (b) a "dog's bone" orbit for  $H \parallel \langle 110 \rangle$ .

ancies have been found for the other metals for which a comparison between theoretical and experimental cyclotron masses is possible (e.g.,<sup>19,36,37</sup> Al). It is believed that these discrepancies are due to effects not included within the framework of the individual electron model, specifically the electron-electron interactions and electron-phonon coupling. As yet the contribution from electron correlations has not been treated adequately for real metals. Studies of the electron-phonon interaction indicate corrections to the masses of the order of magnitude of the discrepancies.<sup>38</sup>

Another noteworthy point about the masses is the relatively small value of the neck mass in comparison to those for orbits on the belly. This fact can be understood in terms of the previously discussed interaction between the conduction and  $d$  bands. As Cohen<sup>39</sup> pointed out, this interaction, which vanishes at  $L$  for the  $L_2'$  state, strongly affects the curvature of the bands in the directions transverse to the neck. The  $s$  level  $L_3$ , which is at a higher energy, does not contribute to the mass for these directions. The effect is important here because of the close proximity of the  $L_3$  ( $d$ -like) and  $L_2'$  levels.

### Optical Properties

In the optical studies of Cu, a sharp rise in the absorption constant which is attributed to interband transitions has been observed to occur at 2.2 eV.<sup>40</sup> These transitions have in the past been interpreted either as transitions from the Fermi level to one of the excited bands<sup>41</sup> or from the  $d$  bands to the Fermi level.<sup>42</sup>

For the theoretical energy bands (shown in Figs. 5 and 6) the lowest energy optical transitions would occur from the  $d$ -band states near the upper  $L_3$  level to the

<sup>36</sup> T. W. Moore and F. W. Spong (to be published).

<sup>37</sup> W. A. Harrison, Phys. Rev. **118**, 1182 (1960).

<sup>38</sup> J. J. Quinn, reference 1, p. 58.

<sup>39</sup> M. H. Cohen, reference 1, p. 176.

<sup>40</sup> S. Roberts, Phys. Rev. **118**, 1509 (1960); L. G. Schulz, *Advances in Physics*, edited by N. F. Mott (Taylor and Francis, Ltd., London, 1957), Vol. 6, p. 102.

<sup>41</sup> For example, see M. Suffczynski, Phys. Rev. **117**, 663 (1960).

<sup>42</sup> N. F. Mott, Phil. Mag. **44**, 187 (1953).

<sup>36</sup> J. M. Ziman, *Electrons and Holes* (Clarendon Press, Oxford, 1960), p. 514.

states at the Fermi level near  $L$ ,<sup>43</sup> which are mainly  $p$ -like. The calculated transition energy is about 2.7 eV for the  $l$ -dependent potential and about 2.1 eV for Chodorow's potential. For *a priori* calculations like the present ones, this agreement with experiment must be considered quite good, particularly as it involves the location of the  $d$  bands. (The nearly perfect agreement for Chodorow's potential is probably fortuitous.)

This good agreement is gratifying as it provides a good deal of confirmation of the general correctness of the calculated  $E(\mathbf{k})$ . For it has been found that the position of the  $d$  bands as a whole, relative to the other bands, is about the most uncertain feature of results. The positions of the  $d$  levels with respect to each other, for example, are given with much less uncertainty. A similar statement holds for the conduction band states except for the shifting of some conduction band states due to the interaction with the  $d$  bands.

At frequencies much lower than those associated with interband transitions, the real part of the dielectric constant,  $\epsilon(\omega) = \epsilon_1(\omega) + i\epsilon_2(\omega)$  can be shown to have the form  $\epsilon_1(\omega) = A - \omega_p^2/\omega^2$  if  $\omega\tau \gg 1$ , where  $\tau$  is the relaxation time. In analogy with the case of free electrons an optical effective mass  $m_{op}$  is defined by the relation  $\omega_p^2 = 4\pi e^2 N_c m_{op}^{-1}$ , where  $N_c$  is the density of conduction band electrons. This mass in turn is related to the band structure by<sup>44</sup>

$$\frac{1}{m_{op}} = \frac{2}{3(2\pi)^3 \hbar^2 N_c} \int d^3\mathbf{k} \nabla_{\mathbf{k}}^2 E(\mathbf{k}) = \frac{2}{3(2\pi)^3 N_c \hbar} \int dS |\mathbf{v}(\mathbf{k})|, \quad (4)$$

where the first integral is over the occupied conduction band states and the second integral is over the Fermi surface.

As mentioned in the discussion of cyclotron resonance, we have only computed the velocity for a few lines and points on the Fermi surface and so cannot directly carry out the surface integral. However, we have already noted that the velocity on the belly appears to be relatively constant except near the neck. The velocity on the neck is obtained from the results illustrated in Figs. 10 and 11 and from the fact that necks are nearly cylindrically symmetric [see Eq. (1)]. Using the above facts and again approximating the belly by a sphere with an average radius, the integral can be readily evaluated. We then find for the optical mass the values  $(1.36 \pm 0.1)m_0$  and  $(1.3 \pm 0.1)m_0$  for the cases of Chodorow's and the  $l$ -dependent potential, respectively. In comparison the experimental value is  $(1.44 \pm 0.01)m_0$ .<sup>40</sup> The comments made concerning the

discrepancies between band theory and experiment for the cyclotron masses are pertinent here.

### Specific Heat

The electronic contribution to the specific heat of a normal metal at low temperature varies linearly with temperature,  $C_{el} = \gamma T$ , with the constant  $\gamma$  being given by

$$\gamma = \frac{1}{3} \pi^2 k^2 N(E_F). \quad (5)$$

The density of states at  $E = E_F$ ,  $N(E_F)$ , is related to the band structure by the well-known relation

$$N(E_F) = \frac{2}{(2\pi)^3} \int \frac{dS}{|\text{grad}_{\mathbf{k}} E(\mathbf{k})|}, \quad (6)$$

where the surface integral is taken over the Fermi surface. Alternatively,  $N(E_F)$  can be expressed as

$$N(E_F) = \frac{2}{(2\pi)^3} \left. \frac{\partial V_k(E)}{\partial E} \right|_{E_F}, \quad (7)$$

where  $V_k(E)$  represents the volume enclosed by a constant energy surface.

The experimental values of  $\gamma$  are customarily expressed in terms of a specific heat effective mass,  $m_T$ , which is defined by

$$\gamma/\gamma_0 = m_T/m_0, \quad (8)$$

where  $\gamma_0$  and  $m_0$  are the free-electron values of the two constants.

Equation (7) is a particularly convenient form for our present purpose as we have already determined the volume as a function of energy in order to find the Fermi energy. Using this, we obtain for the specific heat mass the value  $m_T = (1.17 \pm 0.06)m_0$  for Chodorow's potential and  $(1.12 \pm 0.06)m_0$  for the  $l$ -dependent potential. The measured value of  $m_T$  is  $(1.38 \pm 0.01)m_0$ .<sup>45</sup> The discrepancy between the band theoretical and experimental results is roughly the same as for the cyclotron resonance masses, presumably for similar reasons.

From these results and from our values of the optical mass,  $m_{op}$ , we can see that the ratio  $m_T/m_{op}$  is definitely less than unity. This is in accord with Cohen's<sup>44</sup> inequality for the case of a Fermi surface having an appreciable area of contact with the zone surface.

### V. SUMMARY AND DISCUSSION

This theoretical study of the electronic structure of Cu was undertaken with two principal aims in mind. First, we wished to see if, as has been widely contended, calculated energy bands of Cu are so sensitive to the details of the potential that they would be of doubtful

<sup>43</sup> One can note from Figs. 5 and 6 that an allowed transition between the  $\Delta_5$   $d$  levels and the  $\Delta_1$  state on the Fermi surface would occur for very nearly the same energy as for the transitions at  $L$ . However, states from this region of the zone contribute much less to the combined density of states than the states near  $L$ .

<sup>44</sup> M. H. Cohen, Phil. Mag. **49**, 762 (1958).

<sup>45</sup> W. S. Corak, M. P. Garfunkel, C. B. Satterthwaite, and A. Wexler, Phys. Rev. **98**, 1699 (1955); J. A. Rayne, Australian J. Phys. **9**, 189 (1956).

TABLE V. Comparison of the calculated cyclotron resonance, electronic specific heat, and optical masses with the values obtained from experiment. The calculated masses are given for the band structures based on the two potentials discussed in the text. The tabulated values are in units of the free-electron mass.

Type of mass	Masses, present potential	Masses, Chodorow's potential	Experimental masses
Cyclotron resonance for:			
"belly" orbit, $H\parallel(100)$	$1.1 \pm 0.1$	$1.2 \pm 0.1$	$1.38 \pm 0.01^a$
"dog's bone" orbit	$1.12 \pm 0.06$	$1.13 \pm 0.06$	$1.23 \pm 0.01^a$
"neck" orbit	$0.41 \pm 0.02$	$0.39 \pm 0.02$	$0.6^a$
Specific heat	$1.12 \pm 0.06$	$1.17 \pm 0.06$	$1.38 \pm 0.01^b$
Optical	$1.3 \pm 0.10$	$1.36 \pm 0.1$	$1.44 \pm 0.01^c$

<sup>a</sup> See reference 11.

<sup>b</sup> See reference 45.

<sup>c</sup> See reference 40.

value in the understanding of the metal's physical properties. If this contention could be shown to be incorrect, we then wished to see just how well the resulting energy band structure would agree with the empirical knowledge of it. In view of the fact that the electronic structure of Cu in the vicinity of the Fermi surface is better known experimentally than for any other metal, Cu is, at present, the best metal on which to test the validity of the individual-electron approach.

The manner in which the first problem was studied was to determine the energy bands for two different potentials. The first  $V(\mathbf{r})$  was one originally set up by Chodorow. In it the forces are taken to be the same for all values of the orbital angular momenta,  $l$ , with the forces for  $l=2$  being given most accurately. The second potential is one in which an attempt was made to more properly reflect the variation in the fields for different  $l$  values.

Our results for Chodorow's potential were shown to be in excellent agreement with Chodorow's values which were restricted to the energies for the symmetry points  $\Gamma$ ,  $X$ , and  $L$ . His work was carried out by the augmented plane wave method, while in the present work, the Green's function method was employed. While both methods have already been independently checked, this comparison provides an interesting cross check.

The more interesting and important comparison, however, is between our eigenvalues for the two different potentials. The  $E(\mathbf{k})$ 's for both cases (see Figs. 5 and 6) are shown to be entirely similar throughout the Brillouin zone for the levels in the  $d$  band, conduction band, and low-lying excited band regions. By this we mean that the orderings of the levels for the different  $\mathbf{k}$ 's in the zone are identical and the energy separations of the states are comparable for the two sets of results. From this we can infer that the physical properties derived from these energy bands would be very similar for the two band structures—a fact that was borne out in the investigations of a number of the properties. The important implication of this is that, contrary to the widely-held belief, the  $E(\mathbf{k})$  for Cu and similar metals are not so sensitive to the details of the crystal potential that meaningful calculations for them

cannot be carried out. Of all the features of the band structure, we have found that the position of the  $d$  bands as a whole is the most sensitive to modifications of the fields. The spacing of the levels within these bands is relatively invariant with respect to these changes. From this work, and a comparison with earlier studies, we believe the discrepancies that have appeared in the literature on this metal must have arisen from inadequate solutions of the band problem and not from small differences in the potentials.

The second aspect of this work concerns the study of the extent to which these results agree with the vast amount of information about Cu that has been obtained from experiments. It has been shown that the Fermi surfaces associated with both of the calculated sets of energy bands are in fairly good accord with the experimentally determined one. The theoretical Fermi surfaces intersect the hexagonal zone surfaces as observed, and the radii of the intersection are in good agreement with the measured value. Further, the theoretical results indicated that the main part of the constant energy surface, the so-called belly, deviates from sphericity to a much larger degree than was previously believed. These large deviations have recently been observed by magnetoacoustic effect measurements.

From the calculated  $E(\mathbf{k})$  the energy at which the interband optical transitions commence can be determined and the nature of the transitions ascertained. It is found that the transitions are between the  $d$ -band states near the upper  $L_3$  level and  $p$ -like states of the Fermi surface near  $L_2$ .<sup>43</sup> The energy for the onset of the transitions is given fairly accurately by the energy bands for both potentials. This agreement provides additional confirmation of the correctness of the calculated bands as it shows that the position of  $d$  bands with respect to the other bands is given correctly. As we have mentioned above, the location of the  $d$  bands as a whole is generally the least certain feature of the  $E(\mathbf{k})$  for metals with high-lying  $d$  bands.

We have also considered the cyclotron resonance (for a few specific orbits on the Fermi surface), the specific heat, and the long-wavelength behavior of the dielectric constant for the two band structures. The masses defined in terms of these properties have been calculated

and are all less than the corresponding quantities determined from experiments by about 10 to 30%. (See Table V.) The agreement is thus only semi-quantitative. Similar discrepancies have been found for the other metals for which a comparison between theory and experiment have been made. The discrepancies between the band-theoretical and experimental masses are believed to be due to effects not included in the individual-electron model—specifically, the electron-electron correlations and the electron-phonon coupling. The problem of how the many-electron effects contribute to these masses for a real metal is as yet unsettled. For the electron gas the correlations do not alter the cyclotron<sup>46,46a</sup> or optical masses<sup>47</sup> but do change the specific heat mass,<sup>48</sup> at least in the high-density limit. The contribution of the electron-phonon coupling has been estimated to be about the magnitude of the discrepancies noted above.<sup>38</sup>

A comparison of the calculated bands with soft x-ray studies would be desirable; however, the experimental situation appears to be unclear.<sup>49</sup> The data of Cauchois<sup>50</sup> show a peak having a width of roughly 4 eV. If this is interpreted as being due only to the  $d$  bands it would be in accord with the present work (for which widths of 3.5 eV and 4.1 eV have been found); but this is an admittedly tentative interpretation.

In addition to the above, this work has helped provide an increased understanding of the effects that relatively high-lying  $d$  bands have on the conduction bands. It has been shown how the “interaction” between these bands has led to appreciable distortions of the belly of the Fermi surface. This effect also plays a role in bringing about the contact of the Fermi surface with the zone boundary (see Fig. 8).

Finally, we would like to summarize the limitations of the present work. The first and least serious approximation of all was that the  $V(\mathbf{r})$  was taken to be of the “muffin-tin” potential form. We have calculated the perturbations of the  $s$ - and  $p$ -like levels at  $L$  and  $X$  due to this, and have shown that they are quite small, being  $<0.005$  ry. The perturbations of the  $d$  levels are even

smaller than these. The other approximation, still within the individual particle framework, was the use of potentials which were not shown to be self-consistent. That is, the solutions were not used to construct new potentials from which new solutions are sought, and so forth. The other limitations are those common to all band calculations. They are, as has already been noted, the neglect of the many-electron effects and the electron-phonon coupling.

It is very difficult to estimate the magnitude of the errors involved in not using a self-consistent potential and in employing the individual particle model for a particular physical property. However, since the potentials employed were reasonable and since there was a relatively wide area of agreement between the calculated results and those of experiment, it would appear that the errors attributable to not having a self-consistent potential are not too large. As already mentioned, it is believed that the discrepancies between the calculated and the observed masses are due to the limitations of the individual electron model.

*Note added in proof.* Shoenberg (private communication) has recently revised the previously published de Haas-van Alphen data on which the “experimental” dimensions of the Fermi surface listed in Table IV are based. The revised data, which are in much better accord with the present theoretical results, removes the discrepancy discussed in Sec. III.

An analytical expression for the Fermi surface, which has the form of the first several terms of the tight-binding approximation, has been fitted to Shoenberg’s revised data and, in addition, to Pippard’s<sup>10</sup> anomalous skin effect data by D. J. Roaf (private communication). The resulting surface has been compared to the two surfaces discussed in this work, and it is found that the “empirical” and present theoretical surfaces are quite similar.

It is interesting to note that apparently the two surfaces, the present and the one constructed earlier by Pippard, which has a more spherically symmetric belly, equally well fit Pippard’s data. With the removal of this seeming discrepancy with Pippard’s data, it appears that the shape of the present theoretical surface is in satisfactory agreement with the data from all the principal experiments bearing on the shape.

#### ACKNOWLEDGMENTS

I wish to express my appreciation to Miss E. L. Kreiger for her invaluable assistance with the numerical computations, and to Dr. F. S. Ham and Dr. M. Saffren for comments.

<sup>46</sup> W. Kohn, Phys. Rev. **123**, 1242 (1961).

<sup>46a</sup> Recently Kohn and Luttinger (private communication) have shown that when the skin depth is small compared to the radius of the cyclotron orbit, the interactions do contribute to  $m_e$ . For the electron gas,  $m_e$  is still given by Eq. (2) except that the energy involved includes the effect of the interactions.

<sup>47</sup> D. Bohm and D. Pines, Phys. Rev. **92**, 609 (1953); K. Sawada, K. A. Brueckner, N. Fukuda, and R. Brout, *ibid.* **108**, 507 (1957).

<sup>48</sup> M. Gell-Mann, Phys. Rev. **106**, 369 (1957).

<sup>49</sup> L. G. Parratt, Revs. Modern Phys. **31**, 616 (1959).

<sup>50</sup> Y. Cauchois, Phil. Mag. **44**, 173 (1953).